Available online at www.sciencedirect.com

SciVerse ScienceDirect

Ceramics International 38 (2012) 6041–6045

CERAMICS INTERNATIONAL

www.elsevier.com/locate/ceramint

Short communication

Mechanical properties and microstructures of 2D C_f/ZrC–SiC composites using ZrC precursor and polycarbosilane

Qinggang Li [a,b,c], Shaoming Dong [a,b,*], Ping He [a,b], Haijun Zhou [a,b], Zhen Wang [a,b], Jinshan Yang [a,b,c], Bin Wu [a,b,c], Jianbao Hu [a,b,c]

[a] State Key Laboratory of High Performance Ceramics and Superfine Microstructure, Shanghai Institute of Ceramics, Chinese Academy of Sciences, Shanghai 200050, China

[b] Structural Ceramics and Composites Engineering Research Center, Shanghai Institute of Ceramics, Chinese Academy of Sciences, Shanghai 200050, China

[c] Graduate University of Chinese Academy of Sciences, Beijing 100049, China

Received 23 February 2012; received in revised form 1 April 2012; accepted 2 April 2012

Available online 11 April 2012

Abstract

Two-dimensional C_f/ZrC–SiC composites were fabricated through mold-pressing and polymer infiltration and pyrolysis (PIP) using T700SC plain weave fiber fabrics as reinforcements with ZrC precursor and polycarbosilane. The mechanical properties and microstructures of the composites with 34, 45, and 56% fiber fraction were investigated. All composites showed a typical non-brittle fracture behavior and a large amount of pulled-out fibers were observed on the fracture surface. The bending strength and elastic modulus of the composite with 56 vol% fiber fraction increased up to 582 ± 80 MPa and 167 ± 25 GPa, with increasing fiber fraction. The mass loss and linear recession rate of the composites during the oxy-propane torch test were 0.008 g/s and −0.003 mm/s, respectively. The formation of a $ZrSiO_4$ melt on the surface of the composite significantly contributed to the excellent ablative property of the 2D C_f/ZrC–SiC composites.

Keywords: B. Composites; ZrC precursor; Molding–pressing; Polymer infiltration and pyrolysis

1. Introduction

Carbon fiber-reinforced silicon carbide (C_f/SiC) matrix composites are promising candidates for advanced materials such as gas turbine engines, combustion chambers, thrusters, nozzles, and the noses or leading edges of reentry vehicles because of their excellent toughness, good thermal shock resistance, and good mechanical properties at high temperature [1–3]. Thermal protection systems (reentry vehicles), regardless of their specific designs, require control surfaces with sharp leading edges to enable maneuvering at hypersonic velocities. Low-radius leading edges are subject to significantly greater aerothermal heating than blunt edges, such as those used in space shuttles, reaching temperatures that exceed 2000 °C or above during reentry. Presently available thermal protection materials cannot survive such extreme temperatures, and new materials are required for advanced thermal protection systems.

Carbon–carbon (C/C) composites can be used at temperatures above 3000 °C, which is the temperature used in solid rocket throats; however, their lack of efficient anti-oxidation coating limits their long-term and oxidative-environment use, especially for applications like reusable leading edges [4]. In our previous study, the application of ablation-resistant coatings on the composites significantly improved their ablation resistance at ultra-high temperatures [5]. In addition, replacing the pure carbon or silicon carbide matrices of these composites partly with an ultra-high-temperature matrix would improve the potential application of these composites in extreme environments [6,7]. However, the microstructures of the resulting composites invariably feature ultra-high-temperature ceramic (UHTC) particles, which are introduced through slurry impregnation and are mainly dispersed in the inter-bundle zones.

The current study aims to investigate the properties and microstructures of two-dimensional (2D) C_f/ZrC–SiC composites with different fiber fractions. These composites were

* Corresponding author at: State Key Laboratory of High Performance Ceramics and Superfine Microstructure, Shanghai Institute of Ceramics, Chinese Academy of Sciences, Shanghai 200050, China. Tel.: +86 21 5241 4324; fax: +86 21 5241 3903.

E-mail address: smdong@mail.sic.ac.cn (S. Dong).

0272-8842/$36.00
http://dx.doi.org/10.1016/j.ceramint.2012.04.005

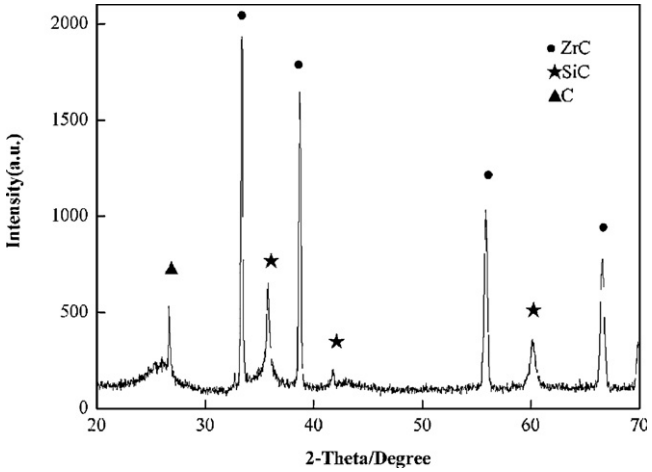

Fig. 1. XRD pattern of the 2D C_f/ZrC–SiC composite.

fabricated via mold-pressing and polymer infiltration and pyrolysis (PIP) using a zirconium (ZrC) precursor and polycarbosilane (PCS).

2. Experimental procedure

T700SC plain woven carbon cloth (Toray, Tokyo, Japan) were used as reinforcements for the composites. The carbon cloth was cut into 100 mm × 90 mm. A PyC/SiC interphase (∼150 nm) was deposited on the fiber cloth via forced pressure-pulsed chemical vapor infiltration (FP-CVI) [8]. Organic Zr-containing polymeric precursors (PZC, Institute of Process Engineering, Chinese Academy of Science, China) were mixed with PCS (National University of Defense Technology, Changsha, China) at a volume ratio of 3:1 and then dispersed in xylene via ultrasonic agitation to form a homogenous mixture. The fiber clothes were then impregnated with the aforementioned mixture and dried. The performs were prepared by stacking these cloths in a graphite die, where the fiber volume fraction was controlled. The graphite die was then heated to approximately 200 °C in a hot-pressing furnace, and pressure (approximately 5 MPa) was applied to control the fiber volume fraction of the samples at a temperature that was slightly higher than the softening temperature of PCS and pyrolyzed for a first time. Further densification was achieved by nine subsequent cycles of impregnation and pyrolysis at 900 °C for 30 min. More detailed experimental procedure was described elsewhere [9–11]. Recently Li et al. [9] reported the properties of the PZC.

Given the complex compositions of the matrices, only the densities and open porosities were measured using the Archimedes' method. The samples were cut and ground into 4 mm × 2 mm × 40 mm specimens for the three-point-bending test, which was performed on an Instron-5566 testing machine, at a crosshead speed of 0.5 mm/min and a span of 24 mm. Six samples were tested in each group of test.

The compositions of the composites were characterized by X-ray diffraction (XRD) with Cu Kα radiation. The microstructures of composites were characterized using Electron Probe Micro-analyzer (EPMA, JXA-800) and Field Emission Transmission Electron Microscopy (FETEM, TEM2010) equipped with an energy dispersive X-ray spectrometer (EDS).

The anti-ablation property test was evaluated according to Test methods for ablation of ablators [The National Military Standard of the People's Republic of China (FL 0183, GJB 323A – 96)]. The anti-ablation property test was conducted using a flowing oxyacetylene torch environment, with approximately 4186.8 ± 418.68 kW/m^2 heat flux and ∼2000 °C flame temperature. The pressures of oxygen and oxyacetylene were 0.4 MPa and 0.095 MPa, respectively, while the gas flow rates were 1512 l/h and 1116 l/h, respectively, and the mixture ration of oxygen and oxyacetylene was 1.35. The surface temperature of the sample was monitored with an optical pyrometer. The 80 mm × 80 mm × 10 mm specimens were mounted in a homemade ultra-high-temperature fixture. The distance from the nozzle tip to the specimen surface was 10 mm, and the inner diameter of the nozzle tip was 2.0 mm. During the test, the ablation gun was ignited firstly. After the flame was steady, the ablation gun was moved vertically to the sample surface, and then the sample was vertically exposed to the flame for 600 s when the surface temperature of the composite reached 1800 °C. The thickness change was measured according to the thickness of the composite in the center of the spot of exposure before and after testing. After testing, the compositions of the composites were characterized by X-ray diffraction (XRD) with Cu Kα radiation.

3. Results and discussion

The XRD pattern of the 2D C_f/ZrC–SiC composite is shown in Fig. 1. Based on the diffraction peaks, the main phases in the

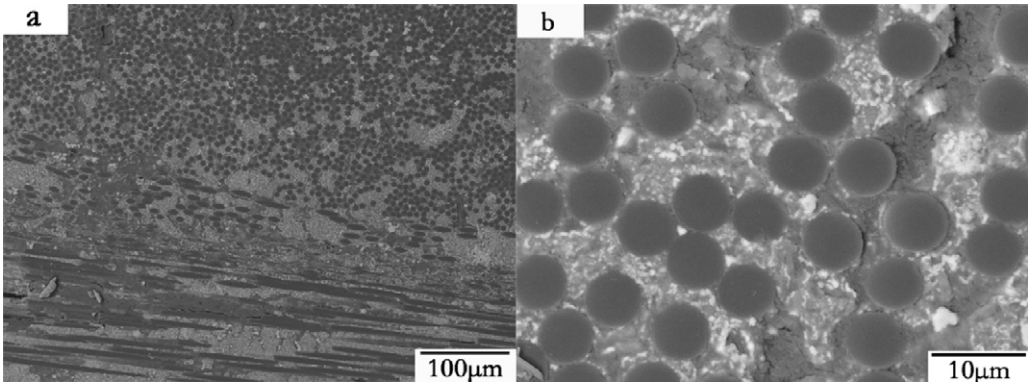

Fig. 2. SEM micrographs of the polished cross-section of the 2D C_f/ZrC–SiC composite: (a) polished cross-sectional image and (b) larger magnification.

composite are carbon fiber, ZrC, and SiC. ZrC is obtained through its precursor, whereas SiC is formed from the pyrolysis of PCS.

The physical and mechanical properties of the 2D C_f/ZrC–SiC composites with different fiber fractions are summarized in Table 1. The bending strength and elastic modulus of the composite with 56 vol% fiber fraction are observed to increase to 582 ± 80 MPa and 167 ± 25 GPa, respectively, with increasing fiber fraction. However, the density decreases as the fiber fraction increases. This composite exhibits a somewhat higher density (2.26 g/cm^3) than those with high fiber fractions (2.17 and 2.13 g/cm^3 for the composites with 45 vol% and 56 vol% fiber fractions, respectively).

The SEM micrographs of the polished cross-section of the 2D C_f/ZrC–SiC composites with 56 vol% fiber fraction are shown in Fig. 2. The use of the PZC and PCS mixture as the precursor results in the filling of the ZrC–SiC nanocomposite matrix with CMCs, leading to the formation of an intra-bundle

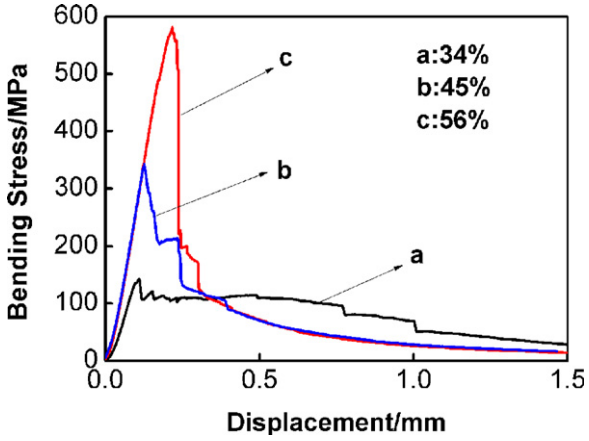

Fig. 3. Bending stress/displacement curves of 2D C_f/ZrC–SiC composites with different fiber fractions.

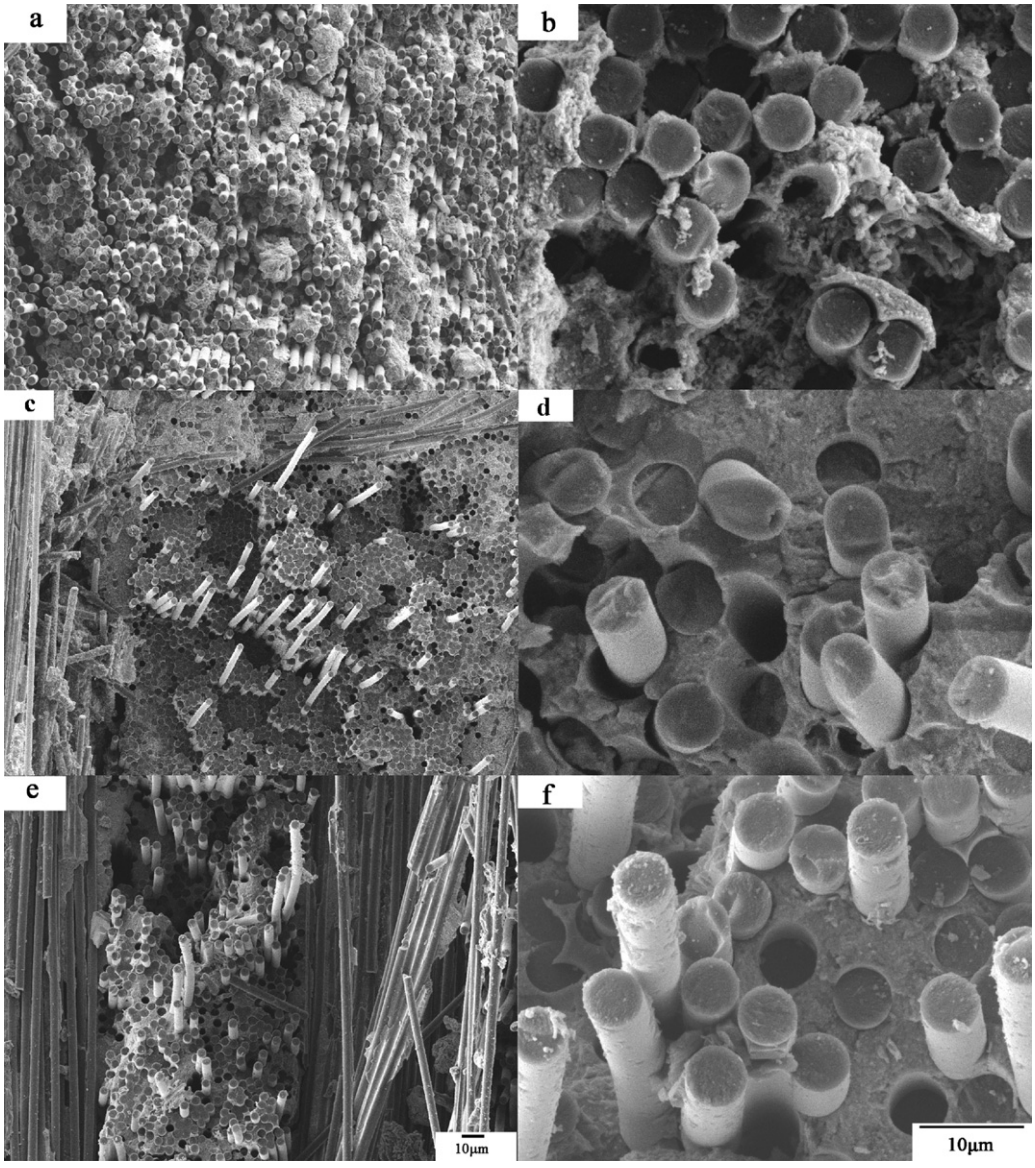

Fig. 4. SEM micrographs of the fracture surfaces of the 2D C_f/ZrC–SiC composites with different fiber fractions: (a, b) 34%; (c, d) 45%; and (e, f) 56%.

Table 1
Properties of the 2D C_f/ZrC–SiC composites with different fiber fractions.

Number	Fiber fraction	ZrC fraction	Density (g/cm^3)	Open porosity	Bending stress (MPa)	Elastic modulus (GPa)
a	34 vol%	34 vol%	2.26	7.2%	143 ± 21	89 ± 33
b	45 vol%	31 vol%	2.17	8.3%	343 ± 26	153 ± 9.0
c	56 vol%	25 vol%	2.13	6.9%	582 ± 80	167 ± 25

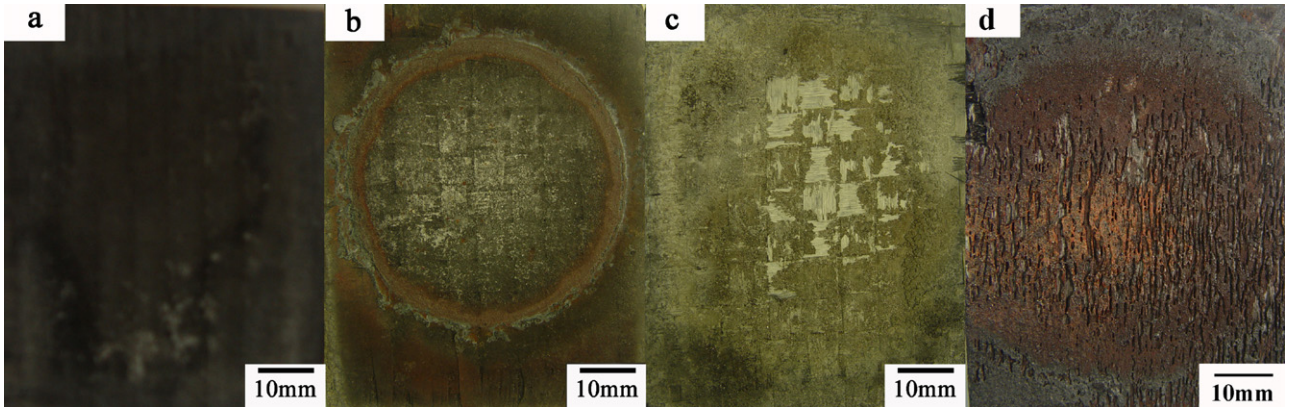

Fig. 5. Anti-ablation property test of the 2D C_f/ZrC–SiC composite: (a) original morphology, (b) front of the composite after testing, (c) back of the composite after testing, and (d) morphology of the C_f/SiC composite after testing.

matrix. The UHTC particles (the ZrC phase) are nearly evenly distributed, but some small pores are evident in the intrabundle areas. The UHTC phase (the ZrC phase, the white background of the micrograph) is homogenously dispersed in the composite.

The bending strength–displacement curves of the composites with different fiber fractions (Fig. 3) show that all composites exhibit a typical non-brittle fracture behavior, as expected. The mechanical properties of the composites, including the elastic modulus and bending strength, significantly increase with increasing fiber fraction.

The morphologies of the fracture surfaces are shown in Fig. 4. All composites exhibit typical non-brittle fracture behaviors, accompanied by fiber pullouts during the fracture process. Moreover, the pulled-out fibers are longer and their surfaces are smoother at 45 vol% and 56 vol% fiber fractions, respectively. However, they are short and has coarse surfaces when the fiber fraction is 34 vol%. This phenomenon can be explained by the bonding strength between fibers and the matrix. When he fiber fraction is 34 vol%, a strong-bonding interface will be produced when the composites are heated at high temperature. As a result, matrix cracks tend to directly penetrate into the fibers with no crack deflection. On the contrary, when he fiber fraction is 45 vol% or 56 vol%, the interphases can result in a weak bonding between fibers and the matrix [12–16], facilitating crack deflection and fiber pulling-out which are beneficial to improvement of fracture toughness. When the fiber fraction is low, the bearing load ability of the composites is descended. As a result, the pulled-out fibers are shorter and their surfaces at 34 vol% fiber fractions are short and coarse.

The 2D C_f/SiC–ZrC composites were exposed to an oxyacetylene torch. The mass loss and linear recession rates are 0.008 g/s and −0.003 mm/s, respectively. Fig. 5 shows the morphologies of the composite surfaces before and after the anti-ablation property test. The morphologies of the composite surface before and after thermal evaluation show that the shape and surface of the composites are retained. A $ZrSiO_4$ glass layer was formed when the composites were used in an oxidative atmosphere. The XRD patterns of the composite surfaces after the anti-ablation property test (Fig. 6) show that the phases include $ZrSiO_4$ and SiO_2. The $ZrSiO_4$ glass layer slows down the speed of oxidation of the composite, thereby contributing to the anti-ablation properties of the 2D C_f/ZrC–SiC composites.

As a comparison, the C_f/SiC composite was tested in the same condition using oxyacetylene torch. Fig. 5d shows the morphology of the C_f/SiC composite surfaces after the anti-ablation property test. Due to the ultra-high-temperature fixture melting, the surface was damaged. But it can be seen from

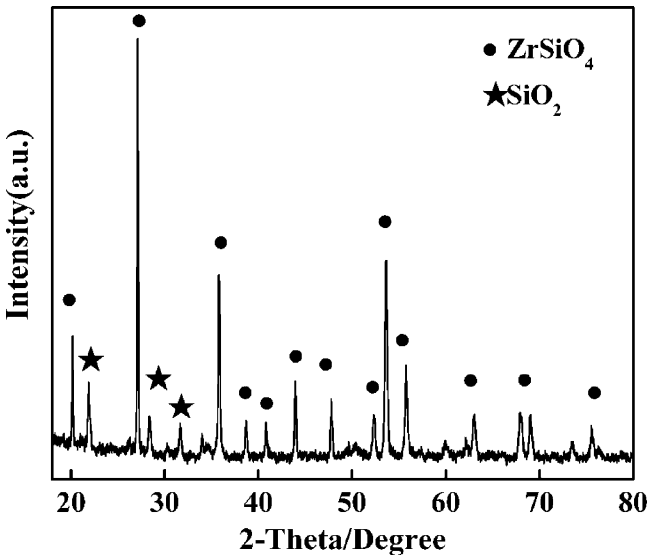

Fig. 6. XRD pattern of the composite surface after the anti-ablation property test.

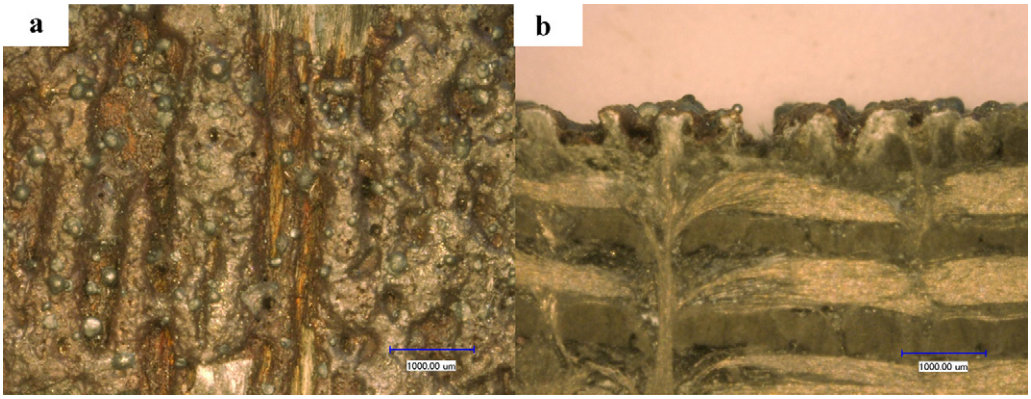

Fig. 7. Morphologies of the C_f/SiC composite after testing: (a) the C_f/SiC composite surface after testing and (b) a section through the center of the C_f/SiC composite after testing.

Fig. 5d that the shape and surface of C_f/SiC composite shows deep pitting because SiC and its ablative product SiO_2 had lower boiling temperatures than the flame temperature and sublimated [17]. Fig. 7 shows the larger magnification of the morphologies of the C_f/SiC composite after testing: (a) the C_f/SiC composite surface after testing and (b) a section through the center of the C_f/SiC composite after testing. The mass loss and linear recession rates are 0.01 g/s and −0.009 mm/s, respectively. As result, the 2D C_f/ZrC–SiC composites have better high-temperature properties than C_f/SiC composites.

4. Conclusions

2D C_f/ZrC–SiC composites were fabricated via mold-pressing and PIP. All composites exhibited typical non-brittle fracture behavior, and a large amount of pulled-out fibers was observed on the fracture surface, and showed a good mechanical properties and an excellent ablative property. In the future, the influence mechanism of the fiber fraction will be investigated. In space re-entry technology for thermal protection is a concept of materials, which during a re-entry are burning off and with comparatively low cost can be re-installed. The thermal protection idea of ceramic matrix composites on the other hand is competing with the cheap ablative materials by the main advantage of being reusable. Thus our future work on 2D C_f/ZrC–SiC composites would be more consistent.

Acknowledgments

Authors appreciate the financial support of the National Natural Science Foundation of China under the Grant No. of 51172256 and Innovation Program of Shanghai Institute of Ceramics Chinese Academy of Sciences under Grant No. of Y12ZC6160G. Authors also thank Professor Xiaolei Wu and Professor Heji Huang from Institute of Mechanics Chinese Academy of Sciences for the plasma wind tunnel test.

References

[1] A. Lacombe, T. Pichon, M. Lacoste, High temperature composite nozzle extensions, a mature and efficient technology to improve upper stage Liquid Rocket Engine performance, AIAA (2007) 2007–5470.

[2] D.P. Stinton, A.J. Caputo, R.A. Lowden, Synthesis of fiber reinforced SiC composites by chemical vapor infiltration, American Ceramic Society Bulletin 65 (2) (1986) 347–350.

[3] S. Schmidt, S. Beyer, H. Knabe, H. Immich, R. Meistring, A. Gessler, Advanced ceramic matrix composite materials for current and future propulsion technology applications, Acta Astronautica 55 (2004) 409–420.

[4] J.C. Han, X.D. He, S.Y. Du, Oxidation and ablation of 3D carbon–carbon composite at up to 3000 °C, Carbon 33 (1995) 473–478.

[5] H.J. Zhou, L. Gao, Z. Wang, S.M. Dong, ZrB_2–SiC oxidation protective coating on C/C composites prepared by vapor silicon infiltration process, Journal of the American Ceramic Society 93 (4) (2010) 915–919.

[6] Z. Wang, S.M. Dong, X.Y. Zhang, H.J. Zhou, D.X. Wu, Q. Zhou, D.L. Jiang, Fabrication and properties of C_f/SiC–ZrC composites, Journal of the American Ceramic Society 91 (10) (2008) 3434–3436.

[7] Z. Wang, S.M. Dong, Y.S. Ding, X.Y. Zhang, H.J. Zhou, J.S. Yang, B. Lu, Mechanical properties and microstructures of C_f/SiC–ZrC composites using T700SC carbon fibers as reinforcements, Ceramics International 37 (2011) 695–700.

[8] Q. Zhou, S.M. Dong, X.Y. Zhang, Y.S. Ding, Z.R. Huang, D.L. Jiang, Synthesis of the fiber coating by FP-CVI process, in: High-Performance Ceramics IV, 2007 Pts 1–3, 336–338, 1307–1309.

[9] Q.G. Li, H.J. Zhou, S.M. Dong, Z. Wang, P. He, J.S. Yang, B. Wu, J.B. Hu, Fabrication of a ZrC–SiC matrix for ceramic matrix composites and its properties, Ceramics International 38 (2012) 4379–4384.

[10] Q.G. Li, S.M. Dong, Z. Wang, P. He, H.J. Zhou, J.S. Yang, B. Wu, J.B. Hu, Fabrication properties of 3-D C_f/SiC–ZrC composites, using ZrC precursor and polycarbosilane, Journal of the American Ceramic Society 95 (4) (2012) 1216–1219.

[11] Q. Li, H. Zhou, S. Dong, Z. Wang, J. Yang, B. Wu, J. Hu, Fabrication a ZrC–SiC matrix for ceramic matrix composites and its properties, Ceramics International (2012), http://dx.doi.org/10.1016/j.ceramint.2012.02.023.

[12] A.G. Evans, D.B. Marshall, The mechanical behavior of ceramic matrix composites, Acta Metallurgica 37 (10) (1989) 2567–2583.

[13] A.G. Evans, D.B. Marshall, F. Zok, C. Levi, Recent advances in oxide–oxide composite technology, Advanced Composite Materials 8 (1) (1999) 17–23.

[14] D.B. Marshall, B.N. Cox, The mechanical of matrix cracking in brittle-matrix fiber composites, Acta Metallurgica 33 (11) (1985) 2013–2021.

[15] M. Kuntz, B. Meier, G. Grathwohl, Residual stress in fiber-reinforced ceramics due to thermal expansion mismatch, Journal of the American Ceramic Society 76 (10) (1993) 2607–2612.

[16] D.B. Marshall, A.G. Evans, Failure mechanisms in ceramic–fiber/ceramic–matrix composites, Journal of the American Ceramic Society 68 (5) (1985) 225–231.

[17] D. Fang, Z. Chen, Y. Song, Z. Sun, Morphology and microstructure of 2.5 dimension C/SiC composites ablated by oxyacetylene torch, Ceramics International 35 (2009) 1249–1253.